

# Advantages of solitonic shape pulses for full-optical wireless communication links

José María Garrido Balsells, Antonio Jurado-Navas\*, Miguel Castillo-Vázquez,  
Ana Belén Moreno-Garrido, and Antonio Puerta-Notario

*Department of Communications Engineering, University of Málaga  
Campus de Teatinos s/n, E-29071 Málaga, Spain*

\*Corresponding author: [navas@ic.uma.es](mailto:navas@ic.uma.es)

Received September 13, 2011; accepted October 20, 2011; posted online December 28, 2011

We propose the use of a power pulse shape of the widely known optical soliton, corresponding to the hyperbolic secant square function, for both conventional atmospheric optical communication systems and, especially, for new full-optical wireless communications. We analyze the performance of the proposed pulse in terms of peak-to-average optical power ratio (PAOPR) and bit error rate (BER). During the analysis, we compare the proposed pulse shape against conventional rectangular and Gaussian pulse shapes with reduced duty cycle. Results show the noticeable superiority of the proposed pulse for atmospheric optical links.

OCIS codes: 010.1300, 010.1330, 060.2605, 290.5930.

doi: 10.3788/COL201210.040101.

In the last few years, the need for achieving inexpensive high-speed links for atmospheric optical communication (AOC) systems has boosted extensive research in infrared wireless communications<sup>[1–4]</sup>. Some of the advantages of AOC systems include ease of deployment, lack of licensing requirements, secure high data rate, and cost-effective wide bandwidth communications. However wireless optical links are affected by fluctuations in both the intensity and the phase of optical waves propagating through this medium<sup>[2]</sup> due to time varying inhomogeneities in the refractive index of the atmosphere. Current AOC systems have developed different techniques to mitigate atmospheric induced effects as, for instance, the inclusion of adaptive optics, the use of large receive apertures, diversity combining schemes, or efficient transmission techniques<sup>[3]</sup>. Following this last strategy, research on free-space optical systems focuses on developing robust techniques, both in transmission and in reception. Particularly, the transmitted pulse shape can be adjusted to the channel conditions, keeping the average optical power transmitted at a constant level as a basic design criterion, due to strict ocular safety international regulations. Based on this idea, the authors proposed transmission schemes with Gaussian pulse shapes with reduced duty cycle to improve the performance of traditional schemes based on rectangular pulses<sup>[5,6]</sup>.

In this letter, we propose the use of an optical pulse based on the power pulse shape of the optical soliton<sup>[7]</sup> for AOC systems. Thus, optical soliton pulse shapes are employed to replace conventional rectangular and Gaussian pulses in wireless optical links, as briefly introduced in Ref. [6]. To show the superiority of the proposed pulse, we analyze the performance of rectangular, Gaussian and solitonic pulses shapes in terms of the peak-to-average optical power ratio (PAOPR) and bit error rate (BER). Note that the PAOPR is a favorable characteristic in intensity-modulation and direct-detection (IM/DD) infrared links that has been analytically corroborated in this letter, due to the inherent features of an IM and the

average power constraints previously mentioned<sup>[5,6]</sup>.

The better behavior of soliton pulses versus Gaussian and rectangular pulses in terms of BER as a direct consequence of having a higher PAOPR justifies its use in wireless optical links. Furthermore, as it is well-known, solitons are stable against perturbations due to local inhomogeneity and noises, so they can be employed as a reliable basis for high bit-rate transmission systems. Both facts are especially relevant in new-generation atmospheric optical systems<sup>[4]</sup> where the optical signal is transparently transmitted from a fiber termination through free space, and then it is coupled into an optical fiber without undergoing any electro/optical conversion in the transceivers. Moreover, these full-optical communication systems are thought to be used as a supplement to other technologies to develop a universal platform to quickly and effectively provide ubiquitous wireless services<sup>[1]</sup>. In this context, soliton pulses can be a promising alternative not only for the fibered part but also, as shown in this letter, for the wireless segment of the link.

Let  $x(t)$  be the instantaneous optical power defined by

$$x(t) = \sum_k a_k \cdot P_{\text{peak}} \cdot p_N(t - kT_b) \quad k \in \mathbf{Z}, \quad (1)$$

where  $a_k$  is a random variable with values of 0 for the bit “0” (off pulse) and 1 for the bit “1” (on pulse),  $P_{\text{peak}}$  is the pulse peak power,  $p_N(t)$  is the pulse shape with normalized peak power, and  $T_b$  is the bit period. Then, the average transmitted optical power can be expressed as  $P = P_{\text{peak}} \cdot P_N \cdot pr(a_k = 1)$ , where  $P_N$  is the optical power averaged over  $T_b$  given by  $P_N = \frac{1}{T_b} \int_0^{T_b} p_N(t) dt$ , and  $pr(a_k = 1)$  is the transmission probability of a bit “1”. Thus, we can write the PAOPR as

$$\text{PAOPR} = \frac{P_{\text{peak}}}{P} = [pr(a_k = 1) \cdot P_N]^{-1}. \quad (2)$$

From Eq. (2), it is deduced that we must reduce  $P_N$ , depending on the adopted pulse shape, to improve the

PAOPR while maintaining the average transmitted optical power at a constant level. Hereafter, to compare the different pulses performance, we define the increase factor in PAOPR as follows:

$$\Gamma_{\text{PAOPR}} = \frac{\text{PAOPR}}{\text{PAOPR}_{\text{ref}}} = \frac{1}{P_{\text{N}}}, \quad (3)$$

where  $\text{PAOPR}_{\text{ref}}$  is the PAOPR obtained with non-return to zero (NRZ) signaling and rectangular pulse shape, i.e.  $P_{\text{Nref}} = 1$ . Note that  $\Gamma_{\text{PAOPR}}$  only depends on the pulse shape characteristics.

Now, we obtain the  $\Gamma_{\text{PAOPR}}$  for the three analyzed pulse shapes: rectangular, Gaussian, and solitonic pulses, all of them depicted in Fig. 1. Firstly, we consider a rectangular pulse with a duty cycle of  $\xi$ , where  $0 < \xi \leq 1$ . In this case, from Eq. (3) it is straightforward derived that

$$\Gamma_{\text{PAOPR}} = \frac{1}{\xi}. \quad (4)$$

Secondly, the expression for a normalized Gaussian pulse shape centered in  $t_0 = \xi T_b/2$  is given by

$$p_{\text{N}}(t) = e^{-(t-t_0)^2/2\sigma_p^2}, \quad (5)$$

where  $\sigma_p = \xi \cdot \sigma_0$  depends on the duty cycle  $\xi$  and on  $\sigma_0 = T_b/n$ , which characterizes the pulse width in relation to the bit period. In particular,  $n$  defines the amount of optical energy contained within  $T_b$ , so that for  $n \geq 6$  at least the 99.8% of the transmitted energy is within  $T_b$ . In our analysis, we assume  $n = 6$  and, thus, the pulse full-width half-maximum (FWHM) expression  $\text{FWHM} = 2\sigma_p\sqrt{2\ln 2}$  is approximately  $0.39\xi T_b$ . From Eqs. (3) and (5) the  $\Gamma_{\text{PAOPR}}$  for the Gaussian pulse is given by

$$\Gamma_{\text{PAOPR}} = \sqrt{\frac{2}{\pi}} \frac{3}{\xi} \left[ \text{erf} \left( \frac{1}{\sqrt{2}} \frac{3}{\xi} \right) \right]^{-1}, \quad (6)$$

where  $\text{erf}(\cdot)$  is the error function.

Regarding the proposed pulse, the expression for a normalized solitonic pulse centered in  $t_0$  is described as

$$p_{\text{N}}(t) = \text{sech}^2 \left( \frac{t-t_0}{\sigma_p} \right), \quad (7)$$

where  $\text{sech}(\cdot)$  denotes the hyperbolic secant function. For this pulse, whenever  $n \geq 8$  at least the 99.9% of the total optical energy is contained within  $T_b$ . In our analysis, we assume  $n = 8$  and, thus, the FWHM, given by  $2\sigma_p \text{asech}(1/\sqrt{2})$ , is approximately  $0.22\xi T_b$ . Note that the proposed pulse shape is remarkably narrower than rectangular and Gaussian pulses, as shown in Fig. 1. For the soliton pulse, the increase factor in PAOPR is obtained from Eqs. (3) and (7) as

$$\Gamma_{\text{PAOPR}} = \frac{4}{\xi} \left[ \tanh \left( \frac{4}{\xi} \right) \right]^{-1}. \quad (8)$$

We can corroborate the higher increase factor in PAOPR for the solitonic pulse in a direct manner. Thus, for a same magnitude of duty cycle, for instance  $\xi = 1$ ,  $\Gamma_{\text{PAOPR}} = 1, 2.4$ , and  $4$ , for a rectangular, a Gaussian,

and a solitonic pulse shape, respectively, concluding that the best performance is expected for the solitonic pulses in relation to the two other remaining pulse shapes.

Now, to verify the superiority of the proposed pulse, we have obtained the error probability for a Gamma-Gamma atmospheric free-space infrared wireless communication system transmitting on-off keying (OOK) formats. As derived in Ref. [8], the Gamma-Gamma probability density function (PDF) of the irradiance  $I$  is given by

$$f_{\text{I}}(I) = \frac{2(\alpha\beta)^{\frac{\alpha+\beta}{2}}}{\Gamma(\alpha)\Gamma(\beta)} I^{\frac{\alpha+\beta}{2}-1} K_{\alpha-\beta} \left( 2\sqrt{\alpha\beta I} \right), \quad (9)$$

where  $K_{\nu}(\cdot)$  is the modified Bessel function of the second kind of order  $\nu$  and  $\Gamma(\cdot)$  is the Gamma function. In Eq. (9), the positive parameters  $\alpha$  and  $\beta$  represent the effective number of large-scale and small-scale cells of the scattering process, respectively<sup>[8]</sup>. From Ref. [2], the total scintillation index  $\sigma_{\text{I}}^2$  is related to these parameters by

$$\sigma_{\text{I}}^2 = \frac{1}{\alpha} + \frac{1}{\beta} + \frac{1}{\alpha\beta}. \quad (10)$$

To obtain the error probability of a link operating in this environment, we must start from the conditional BER (CBER) of the system. Assume an IM/DD scheme using an OOK constellation such that, from Eq. (1),  $x \in \{0, P_{\text{peak}}\}$ , and maintaining the average transmitted optical power,  $E[P]$ , at a same constant level. Hence, from Ref. [2], the CBER is written as

$$P_{\text{b}}(e|I) = \frac{1}{2} \text{erfc} \left( \frac{P_{\text{peak}}RI}{2\sqrt{2}\sigma_{\text{N}}} \right). \quad (11)$$

In this last expression,  $R$  represents the responsivity,  $\sigma_{\text{N}}^2$  is the additive white Gaussian noise variance, whereas  $\text{erfc}(\cdot)$  is the complementary error function. From Eq. (1), the average transmitted power is expressed as:  $P = P_{\text{peak}}P_{\text{N}}pr(a_k = 1)$ . From Eqs. (2) and (3),  $P_{\text{N}} = (\Gamma_{\text{PAOPR}})^{-1}$ , so  $P_{\text{peak}} = P \Gamma_{\text{PAOPR}}/pr(a_k=1)$ . Consequently, the average BER,  $P_{\text{b}}(e)$ , can be obtained by averaging  $P_{\text{b}}(e|I)$  over  $f_{\text{I}}(I)$ , i.e.  $P_{\text{b}}(e) = \int_0^{\infty} P_{\text{b}}(e|I)f_{\text{I}}(I)dI$ , as shown in Ref. [2]. Now we can substitute Eq. (9) in this last equation and express the  $K_{\nu}(\cdot)$  and the  $\text{erfc}(\cdot)$  integrands as Meijer-G functions. In these sense, we employ [9, Eq. (07.34.03.0605.01)] and [9, Eq. (07.34.03.0619.01)], respectively, in a similar way as

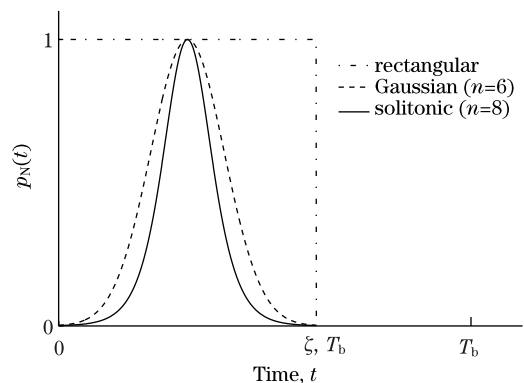


Fig. 1. Optical power pulse shape for different amplitude-normalized pulses,  $p_{\text{N}}(t)$ , with a reduced duty cycle,  $\xi$ .

Ref. [10]. Finally, and by utilizing [9, Eq. (07.34.21.0013.01)], the average BER can be written in a closed-form expression as

$$P_b(e) = \frac{2^{\alpha+\beta-1}}{4\pi\sqrt{\pi}\Gamma(\alpha)\Gamma(\beta)} \times G_{5,2}^{2,4} \left\{ \frac{2(RP\Gamma_{\text{PAOPR}})^2}{\sigma_N^2 [\alpha\beta pr(a_k = 1)]^2} \middle| \begin{matrix} \frac{1-\alpha}{2}, \frac{2-\alpha}{2}, \frac{1-\beta}{2}, \frac{2-\beta}{2}, 1 \\ 0, \frac{1}{2} \end{matrix} \right\}. \quad (12)$$

As can be numerically observed by evaluating the Meijer-G function of Eq. (12), such the  $G$  function decreases as its first argument increases so that the PAOPR relationship is analytically corroborated as a favorable figure of merit in optical environments because an increase in its value involves a lower error probability.

Figure 2 shows some obtained curves of BER from Eq. (12) with the three pulse shapes analyzed in this letter. In this respect, we have supposed that either symbol is equally likely to be transmitted, i.e.,  $pr(a_k = 1) = 1/2$ , whereas the transmitted optical power for every transmitted pulse has been normalized. Consequently, the average transmitted optical power has been fixed to  $E[P] = 1/2$ . In addition, a unity responsivity coefficient,  $R$  is also assumed as well as two different turbulent regimes: first a weak turbulence regime where  $\alpha = 10$  and  $\beta = 5$ , so that, from Eq. (10),  $\sigma_I^2 = 0.32$ ; secondly, a moderate-to-strong irradiance fluctuation regime, where  $\alpha = 2.34$  and  $\beta = 1.18$ , so that  $\sigma_I^2 \approx 2$ .

It is clearly observed that OOK formats with a shortened duty cycle exhibit a greater robustness to adverse conditions. This confirms that an increase in PAOPR leads to a decrease in BER as it is directly observed from Eq. (12). In Fig. 2 it is also shown that the solitonic pulse shape offers a lower BER than conventional rectangular and Gaussian pulses for the simulated

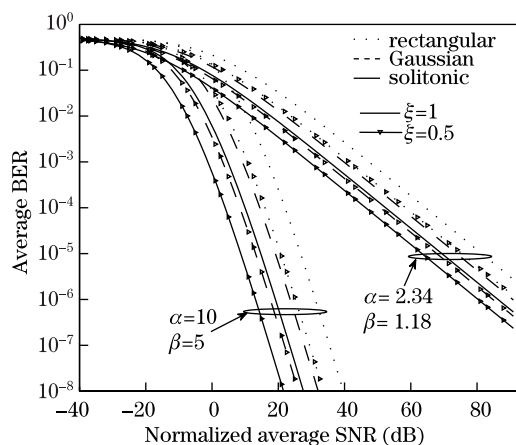


Fig. 2. BER against SNR using different optical pulse shapes and duty cycles. The SNR has been defined as  $10 \log_{10} [P^2 R^2 / (2\sigma_N^2)]$ .

systems, as deduced before from the  $\Gamma_{\text{PAOPR}}$  analysis. For instance, for an error probability of  $10^{-6}$ , a solitonic pulse shape achieves an improvement of 4.47 and 12.07 dB in signal-to-noise ratio (SNR) in relation to the results obtained by a Gaussian and a rectangular pulse shape, respectively. This fact justifies the use of such a proposed pulse in AOC systems and, in addition, in full-optical wireless communication links.

In conclusion, we analyze the behavior of a pulse based on the power pulse shape of the optical soliton for its use in atmospheric wireless optical communications. We analyze and verify the superiority of solitonic pulses against rectangular and Gaussian pulses in terms of PAOPR and BER in AOC systems, leading to practical considerations in terms of designing hybrid fiber and wireless optical communications systems. Finally, although advantages of soliton pulses in optical fiber transmissions are well-known<sup>[11]</sup>, to the best of our knowledge, it is the first time that performance of optical solitons in AOC links is shown.

This work was fully supported by the Spanish Ministerio de Ciencia e Innovacion (MICINN) under Grant No. TEC2008-06598.

## References

1. K. Kazaura, K. Wakamori, M. Matsumoto, T. Higashino, K. Tsukamoto, and S. Komaki, *IEEE Commun. Mag.* **48**, 130 (2010).
2. L. C. Andrews, R. L. Phillips, and C. Y. Hopen, *Laser Beam Scintillation with Applications* (Bellingham, Washington, 2001).
3. M. Razavi and J. H. Shapiro, *IEEE Trans. Wire. Commun.* **4**, 975 (2005).
4. M. Matsumoto, K. Kazaura, P. Dat, A. Shah, K. Omae, T. Suzuki, K. Wakamori, T. Higashino, K. Tsukamoto, and S. Komaki, in *Proceedings of the First ITU-T Kaleidoscope Academic Conference, Innovations in NGN (K-INGN 2008)* 221 (2008).
5. J. M. Garrido-Balsells, A. García-Zambrana, and A. Puerta-Notario, *IEE Electron. Lett.* **42**, 43 (2006).
6. A. Jurado-Navas, J. M. Garrido-Balsells, M. Castillo-Vázquez, and A. Puerta-Notario, *Opt. Express* **18**, 17346 (2010).
7. Y. S. Kivshar and G. P. Agrawal, *Optical Solitons: From Fibers to Photonic Crystals* (Academic Press, Amsterdam, 2003).
8. M. A. Al-Habash, L. C. Andrews, and R. L. Phillips, *Opt. Eng.* **40**, 1554 (2001).
9. The Wolfram functions site (2001), <http://functions.wolfram.com>.
10. T. A. Tsiftsis, *IET Electron. Lett.* **44**, 373 (2008).
11. A. Hasegawa, *IEEE J. Sel. Top. Quantum Electron.* **6**, 1161 (2000).